Synergistic inhibition of ovarian cancer cell growth by combining selective PI3K/mTOR and RAS/ERK pathway inhibitors.

Karen E. Sheppard[1,6,7], Carleen Cullinane[4], Katherine M. Hannan[1], Meaghan Wall[1], Joanna Chan[1], Frances Barber[1], Jung Foo[1], Donald Cameron[1], Amelia Neilsen[1], Pui Ng[1], Jason Ellul[1], Margarete Kleinschmidt[1], Kathryn M. Kinross[1,6], David D. Bowtell[2,6,8], James G. Christensen[9], Rodney J. Hicks[4,6], Ricky W. Johnstone[3,6], Grant A. McArthur[1,3,4,6,8], Ross D. Hannan[1,6,7,10,11], Wayne A. Phillips[5,6] and Richard B. Pearson[1,6,7]*

[1]Oncogenic Signalling and Growth Control, [2]Cancer Genomics, [3]Cancer Therapeutics Program, [4]Translational Research Laboratory and [5]Surgical Oncology, Peter MacCallum Cancer Centre, Locked Bag 1, A'Beckett St, Melbourne, Victoria 8006, Australia.

[6]Sir Peter MacCallum Department of Oncology, [7]Department of Biochemistry and Molecular Biology, and [8]Department of Pathology, University of Melbourne, Parkville, Victoria 3010, Australia.

[9]Pfizer Corporation, La Jolla, California, USA.

[10]Department of Biochemistry and Molecular Biology, Monash University, Clayton, Victoria 3800, Australia.

[11]School of Biomedical Sciences, University of Queensland, Queensland 4072, Australia

RUNNING TITLE: Targeting the PI3K and RAS pathways in ovarian cancer

KEY WORDS: Ovarian Cancer, PI3 Kinase, RAS/ERK Pathway, therapeutics

*CORRESPONDING AUTHOR: Richard B. Pearson, Peter MacCallum Cancer Centre, Locked Bag 1, A'Beckett St. Melbourne, Victoria 3000, Australia. rick.pearson@petermac.org Phone +61396561247 Fax +61396563537

DISCLOSURE OF POTENTIAL CONFLICTS OF INTEREST: J. Christensen: employee and shareholder, Pfizer.

Abstract

Background: Ovarian cancer is the major cause of death from gynecological malignancy with a 5 year survival of only ~30% due to resistance to platinum and paclitaxel-based first line therapy. Dysregulation of the PI3K/mTOR and RAS/ERK pathways is common in ovarian cancer, providing potential new targets for 2nd line therapy.

Methods: We determined the inhibition of proliferation of an extensive panel of ovarian cancer cell lines, encompassing all the major histotypes, by the dual PI3K/mTOR inhibitor PF-04691502 and a MEK inhibitor, PD-0325901. In addition, we analysed global gene expression, mutation status of key PI3K/mTOR and RAS/ERK pathway members and pathway activation to identify predictors of drug response.

Results: PF-04691502 inhibits proliferation of the majority of cell lines with potencies that correlate with the extent of pathway inhibition. Resistant cell lines were characterized by activation of the RAS/ERK pathway as indicated by differential gene expression profiles and pathway activity analysis. PD-0325901 suppressed growth of a subset of cell lines that were characterized by high basal RAS/ERK signalling. Strikingly, using PF-04691502 and PD-0325901 in combination resulted in synergistic growth inhibition in 5/6 of PF-04691502 resistant cell lines and 2 cell lines resistant to both single agents showed robust synergistic growth arrest. Xenograft studies confirm the utility of combination therapy to synergistically inhibit tumour growth of PF-04691502-resistant tumours *in vivo*.

Conclusions: These studies identify dual targeted inhibitors of PI3K/mTOR in combination with inhibitors of RAS/ERK signalling as a potentially effective new approach to treating ovarian cancer.

1. Introduction

Ovarian cancer has the highest mortality rate among all gynecological cancers [1] largely due to the late diagnosis. Most patients respond to debulking surgery and treatment with a combination of taxane and platinum-based therapy, but later develop disease recurrence due to intrinsic and acquired resistance. Thus novel strategies are required to better treat this disease at diagnosis and/or provide an effective second line treatment. Dysregulation of both the PI3K pathway and RAS/ERK pathway are highly prevalent in all histotypes of ovarian cancer and hence targeting these pathways may provide a novel alternative to conventional therapy. [2-5]

PI3K initiates a signalling cascade that activates mTORC1 via AKT and subsequent phosphorylation of many factors that impact on cell metabolism, angiogenesis, cell growth, proliferation and survival. [6-8] RAS signalling via RAF and MEK leads to the activation of both extracellular signal-related kinase (ERK) 1 and ERK2. ERK phosphorylates several cytosolic and nuclear proteins, including transcription factors that regulate the cell cycle. [9] Currently, inhibitors of RAF and MEK are the most advanced in the clinic for blocking ERK signalling, [10, 11] while for the PI3K pathway there are many agents targeting different members of the pathway (PI3K, AKT, mTORC1, mTOR) including some that inhibit multiple components (PI3K and mTOR). [12] The dual PI3K and mTOR inhibitors have shown great promise in preclinical models. [13] PF-04691502 (PF502) is an ATP-competitive inhibitor of PI3K and both mTOR complexes [14] and is currently in several clinical trials [15], PD-0325901 (PD901) is a selective inhibitor of both MEK isoforms (MEK1/MEK2) and thus prevents activation of ERK and is also currently in a clinical trial. [16]

Given the high frequency of activating events in both the PI3K and RAS pathways we sought to determine the efficacy of PF502 and PD901 on a panel of 30 ovarian tumour cell lines. In addition, we performed global mRNA expression profiling, complemented with targeted mutation and pathway activity analysis to identify potential predictive and response biomarkers. These analyses identified RAS signalling as a key mediator of PF502 resistance and established the rationale for combination therapies with PF502 and PD901 in ovarian cancer.

2. Materials and Methods

2.1.Cell Lines

Individuality of ovarian cell lines listed in Supplementary Table S1 was routinely confirmed by a PCR based short tandem repeat (STR) analysis using 6 STR loci.

2.2.Therapeutics

2-amino-8-[trans-4-(2-hydroxyethoxy)cyclohexyl]-6-(6-methoxypyridin-3-yl)-4-methylpyrido[2,3-d]pyrimidin-7(8H)-one (PF-04691502) [14] and *N*-[(2R)-2,3-dihydroxypropoxy]-3,4-difluoro-2-[(2-fluoro-4iodophenyl)amino]-Benzamide (PD-0325901) [17, 18] were obtained from Pfizer Oncology.

2.3.Cell Proliferation Assay

Cells were drug treated for 72hrs, and cell number assessed via an imaging system (Incucyte, Essen Instruments) or the sulforhodamine B assay; cells were less than 90% confluent in control wells at the end of incubation. GI50 was determined using GraphPad Prism. For PF502, GI50 values followed a Gaussian distribution so the mean (232nM) of all 30 cells was used to define cells as resistant or sensitive. For PD901, as the GI50's did not follow a Gaussian distribution the geometric mean (1.21 μM) was used to define cells as resistant or sensitive.

To assess drug synergy dose response curves were generated for both single agents and their combination. A mutually nonexclusive combination index (CI) was determined using CalcuSyn (Biosoft) where: CI<1 synergy; CI>1 antagonism; CI=1 additive. [19] The combination ratio was fixed and based on the GI50 for each drug, where the highest and

lowest combination ratio was 8 times and 1/8th the GI50, respectively. Cell lines resistant to PD901 were treated with a fixed concentration of 100nM PD901 in combination with a dose range of PF502.

2.4.Cell Death Assay

Cell death was determined using propidium iodide (PI) staining followed by flow cytometry (LSRII) and data analyzed using FCS express software (De Novo Software).

2.5.Immunoblotting

Cells were lysed in RIPA buffer, subjected to SDS-PAGE, immunoblotted, and protein bands visualized and quantified (ImageQuant :GE Healthcare: Supplementary Methods) .

2.6.Gene Expression

Cells were harvested at 50-80% confluency. RNA was extracted (QIAGEN RNeasy kit), *in vitro* transcribed and biotin labelled cRNA was fragmented and hybridized to Affymetrix 1.0ST expression array as per manufacturer's instructions (accession number GSE43765). Differential gene expression was determined using the Limma R package after RMA normalization and background correction. [20] Genes that had a >1.4 fold change in expression between resistant and sensitive were included in the MetaCore pathway analysis (http://thomsonreuters.com/metacore).

2.7.Gene Mutational Analysis

Genomic DNA was extracted using the QIAamp DNA Blood Mini kit (QIAGEN). PCR primers and annealing temperatures are in Supplementary Table S2. Cycle sequencing

was performed using the BigDye Terminator v3.1 Cycle Sequencing Kit and analyzed on a 3130 Genetic Analyzer (Applied Biosystems).

2.8.Human Ovarian Cancer Xenograft Assays

Female Balb/c nude mice were injected subcutaneously with $5x10^6$ cells in 0.05mL of 50% Matrigel. When tumours reached ~$100mm^3$, mice were randomized into groups of 10 and daily oral gavaged with vehicle, 10mg/kg PF502, 1mg/kg PD901 or PF502 plus PD901. For immunoblotting, tumours were frozen and protein extracted from 4 mice, 4hrs after a single drug treatment. (21)

2.9.Gene Set Enrichment Analysis

For Gene Set Enrichment Analysis (GSEA) 1,000 iterations were performed using the default weighted enrichment statistic and a signal-to-noise metric to rank genes based on their differential expression across sensitive and resistant cell lines. (22)

2.10.Statistical Analysis

Student's t-test or one-way analysis of variance followed by Tukey's Multiple Comparison Test was performed using GraphPad PRISM. To calculate the correlation between two variables a two-tailed Spearman correlation test was performed. Chi-square tests were used to assess associations between mutation status and sensitivity. Differences of $p<0.05$ were considered significant. All data are expressed as mean $\pm$ SEM.

3. Results

3.1.PF502 and PD901 inhibit ovarian cancer cell proliferation

The PF502 concentration, that inhibited proliferation by 50% (GI50) ranged from 16nM to 640nM (Fig. 1A) whereas response to PD901 showed a bimodal pattern, with a subset of cells that were highly sensitive (GI50's 3nM to 300nM: Fig. 1B). All cell lines showed sensitivity to at least one of the two agents.

3.2.PF502 and PD901 induces cell death

PF502 induced cell death in all cell lines and significantly correlated (Spearman correlation test $r = -0.66$, $p<0.0001$) with the drugs ability to inhibit cell proliferation (Fig. 1C). In contrast, in PD901 sensitive cells there was minimal cell death and even less in resistant cell lines (Fig. 1D).

3.3.PF502 inhibits PI3K/AKT/mTOR pathway signalling

To assess if PF502 was effectively inhibiting its targets a subset of sensitive and resistant cell lines were treated with either 100nM or 1μM PF502 and phosphorylation of components of the PI3K/mTOR pathway measured. Phosphorylation of PRAS40 (P-PRAS) was used as a measure of AKT activity, P-AKT (S473) as a measure of AKT and mTORC2 activity, and both P-rpS6 and P-4EBP1 as a measure of mTORC1 activity. At 100nM, PF502 decreased the phosphorylation of all proteins measured and was a highly potent inhibitor of AKT phosphorylation in PF502 sensitive compared to resistant cell lines (Fig. 2). The response to PF502 in resistant cell lines of all phospho-proteins measured was less robust indicating that resistance is associated with the inability of PF502 to effectively inhibit PI3K/AKT/ mTORC1 signalling.

3.4.PD901 effectively inhibits MEK activity in resistant and sensitive cells.

To assess if PD901 effectively inhibited MEK activity we treated cells with either 100nM or 1μM PD901 and determined phosphorylation of ERK (P-ERK) in a subset of resistant and sensitive cell lines. P-ERK was completely inhibited with 100nM PD901 in both resistant and sensitive cell lines (Fig. 3), demonstrating that drug resistance was not due to failure to inhibit MEK.

3.5.PI3K & RAS/ERK pathway analysis in ovarian cancer cell lines

To evaluate if the activation state of PI3K or RAS/ERK pathways influence ovarian cancer cell sensitivity to PF502 and/or PD901 we determined PTEN protein levels, activating mutations in PIK3CA, AKT1, BRAF and KRAS genes and then correlated these results with sensitivity to the inhibitors. 25 cell lines (83%) expressed <50% PTEN protein compared to HOSE (Fig 4.B), 6 cell lines (20%) had activating mutations in the PIK3CA gene, 5 cell lines (17%) had activating mutations in either BRAF or KRAS and no mutations in AKT1 were detected (Fig.4A). Loss of PTEN protein or PIK3CA mutations did not correlate with either sensitivity to PF502 or resistance to PD901. However, activating KRAS or BRAF mutations were associated with increased resistance to PF502 (4/5 cell lines with mutations were resistant: Fig. 4A), and all cell lines with these mutations were sensitive to PD901.

PI3K and RAS/ERK pathway activation was further assessed by measuring P-PRAS40, P-rpS6 and P-ERK (Fig. 4B). P-PRAS40 was elevated in 16 (53%) of ovarian cancer cell lines, however, consistent with the genomic analysis, there was no correlation with P-PRAS levels and sensitivity to PF502 or resistance to PD901, suggesting that elevated

AKT activity does not affect sensitivity to either of these inhibitors. Importantly however, increased P-rpS6 levels and P-ERK correlated with resistance to PF502 ($p < 0.02$, Spearman test: Supplementary Fig.S1).

3.6.Differential gene expression between PF502 and PD901 resistant and sensitive cell lines

To identify molecular pathways that may confer sensitivity and/or resistance to either PF502 or PD901 we examined the difference in gene expression between resistant and sensitive cell lines using GSEA and MetaCore pathway analysis. Using GSEA two RAS oncogenic signatures and a “basal” breast cancer phenotype, which is characterized by RAS/ERK activation were enriched in PF502 resistant cell lines (Supplementary Table S3). [23] In contrast, RAS oncogenic signatures and the “basal” breast cancer phenotype, were highly represented in PD901 sensitive cells (Supplementary Table S4). Metacore analysis of differentially expressed genes was also indicative of RAS/ERK activation in PF502 resistant and PD901 sensitive cells, consistent with the GSEA. Furthermore, Metacore analysis implicated cytokine signaling as potentially conferring PF502 resistance, which also may reflect RAS/ERK activation [24] (Supplementary Table S5). These data support the mutational and western analysis that increased signalling in the RAS/ERK pathway correlates with PF502 resistance and PD901 sensitivity. This data suggests that in ovarian cancer cells increased RAS/ERK signalling confers sensitivity to PD901 and reinforces the possibility that PD901 may prove effective in inhibiting the growth of PF502-resistant cell lines.

3.7.PD901 and PF502 synergize in PF502 resistant cell lines

Our protein, mutation and gene expression data all strongly indicate that activation of the RAS/ERK pathway conferred resistance to PF502. Thus we investigated whether dual inhibition of MEK and PI3K/mTOR activity resulted in greater inhibition of proliferation and/or cell death compared to single agent treatment. In 5 of 6 PF502 resistant cell lines a combination of PF502 and PD901 resulted in a synergistic reduction in cell proliferation (mutually nonexclusive CI<1) whilst the other an additive response (CI=1). Importantly, in two PF502 and PD901 resistant cell lines (SKOV3 and JHOC5) there was a robust synergistic response (Fig.5).

3.8.Pre-clinical efficacy studies

To confirm that resistance to PF502 and the synergistic effect with PD901 was relevant *in vivo,* we tested anti-tumour effects in xenografts. ES2 tumours were relatively resistant to PF502 with a small (17±3%) but significant decrease in tumour size following 19 days of treatment, more sensitive to PD901 (37±3% decrease) and more potently inhibited when these compounds are combined (75±3% decrease: Fig.6). Levels of P-AKT were barely detectable in ES2 xenografts, consistent with cell culture data (Fig 2A) however P-PRAS was effectively inhibited by PF502. Importantly PD901 was more effective than PF502 at inhibiting P-rpS6 and the combination was more effective than single agent treatment. Thus decreased P-rpS6 reflected inhibition of tumour growth and that RAS/ERK pathway induced P-rpS6 [25] is associated with PF502 resistance.

In a second human xenograft model using MCAS cells, which *in vitro* were relatively resistant to PF502 but sensitive to PD901, PF502 alone significantly inhibited tumour growth with a 68±3% decrease in tumour size following 19 days of treatment (Supplementary Figure S2). Western analysis demonstrated that PF502 not only

decreased PI3K/mTOR signaling (decreases in P-AKT, P-PRAS and P-S6) but also decreased P-ERK, supporting the hypothesis that inhibition of both PI3K/mTOR and the MAPK/ERK pathways effectively inhibits ovarian tumour growth.

4. Discussion

Both the PI3K/mTOR and RAS/ERK pathways are highly dysregulated through gene amplifications, gene deletions [2] and mutations in all histotypes of ovarian cancer. [5] In this study we analyzed the response of an extensive panel of 32 ovarian cancer cell lines to specific inhibitors of PI3K/mTOR (PF502) and RAS/ERK (PD901) signalling which are currently in clinical trials. The majority of cells showed growth inhibition in response to PF502 while there was a clear division between PD901 sensitive and resistant cell lines with some cell lines not responding at all (up to 30μM).

To identify predictors of drug response, we analyzed global gene expression, mutation and activation status of constituents of the PI3K and RAS/ERK pathways. Historically one of the best predictors of sensitivity to kinase inhibitors has been the presence of an activating mutation or other genomic alterations in the targeted kinase. [26] Our study indicates that increased PI3K pathway signalling in ovarian cancer is unlikely to confer sensitivity to PI3K pathway inhibitors, since PTEN loss or PIK3CA mutations did not correlate with PF502 response. Mutations in PIK3CA and loss of PTEN predict sensitivity to PI3K pathway inhibitors in most [27-29], but not all cases [30] and this may reflect differences in the genetic backgrounds of the tumour cells and/or the specificity of the individual inhibitors. In contrast, mutations in KRAS and BRAF did confer sensitivity to MEK inhibition by PD901, and furthermore GSEA also identified activation of the RAS pathway as conferring

sensitivity. This is consistent with previous studies that demonstrated that mutations in KRAS and BRAF confer sensitivity to MEK inhibition in several different cancer types [31-33] including ovarian. [34]

Identification of predictors of drug resistance will be essential for optimizing treatment regimes. Our analysis focused on signatures of resistance to PF502 given its potency in inhibiting growth of the majority of cell lines. Protein, mutational and genomic analysis implicated activation of the RAS/ERK pathway as conferring PF502 resistance, consistent with similar findings in other systems. [28, 35-37] This resistance is likely due to known effects of the RAS/ERK pathway on rpS6 phosphorylation, translation [25], gene transcription and cell cycle progression. [38] Strikingly, in combination experiments the majority of PF502 resistant cell lines showed a synergistic response when treated with both PF502 and PD901 and this was also evident *in vivo* in the ES2 xenograft model. Importantly, in those cell lines that were resistant to both PF502 and PD901 individually, the combination potently inhibited cell growth. These data suggest that while PI3K/mTOR signalling is vital for ovarian cancer cell proliferation, optimal inhibition of tumour growth will require targeting the PI3K/mTOR and RAS/ERK pathways in combination. Indeed, xenograft studies with the MCAS cell line that was PF502 resistant but PD901 sensitive, revealed *in vivo* sensitivity to single agent treatment with PF502 that correlated with additional inhibition of the RAS/ERK pathway.

P-rpS6 level reflected PF502 efficacy in cell lines and *in vivo* efficacy of PF502, PD901 and their combination, thus is a potential tumor response biomarker. The failure of PF502 to effectively inhibit AKT or mTORC1 activity in resistant cell lines requires further investigation. Cellular availability of PF502 is unlikely the cause as it is not a substrate for

the multidrug resistance protein 1, is not rapidly metabolized [39] and our pathway analysis reveals that in some resistant cell lines the drug is able to effectively inhibit one target but not another. A more likely explanation is that other pathways feed into the PI3K pathway, such as RAS/ERK or DNA-dependent protein kinase both of which can phosphorylate components of the PI3K pathway leading to its activation.[25, 40]

In summary, the majority of ovarian cancer cell lines responded to the PI3K/mTOR inhibitor, PF502 making this a potential novel treatment for ovarian cancer. In contrast, the obvious dichotomy in response to MEK inhibition by PD901 and the correlation of increased signalling in the RAS/ERK pathway with PD901 sensitivity suggests that MEK inhibitors are only likely to be effective as single agents in BRAF and KRAS mutant ovarian tumours. Concomitant inhibition of the MEK and PI3K/mTOR pathways resulted in effective inhibition of cell proliferation and induction of cell death in PF502-resistant cells and inhibited tumour growth *in vivo*, indicating that combination therapy with selective PI3K/mTOR and RAS/ERK pathway inhibitors might provide an effective new treatment option for ovarian cancer. Assessment of the effectiveness of this approach and further definition of signatures of patient response will await future clinical trials.

Acknowledgments:

The authors thank Jeannette Schreuders, Susan Jackson and Ekaterina Bogatyreva for technical assistance. This work was supported by grants from the NHMRC of Australia to KES & RBP (#I043884), RWJ (#251608 & #566702), GAM (#400120 & #566876), RDH (#166908 & #251688), WAP (#628620), RBP (#509087 & #400116), and from Pfizer Oncology. Researchers were funded by NHMRC (Research Fellowships to RWJ, RDH & RBP) and Cancer Council of Victoria (Sir Edward Weary Dunlop Fellowship to GAM).

References:

1. Siegel R, Naishadham D, Jemal A. **Cancer statistics, 2012**. *CA Cancer J Clin*. 2012;62:10-29.
2. TCGA. **Integrated genomic analyses of ovarian carcinoma**. *Nature*. 2011;474:609-615.
3. Singer G, Oldt R, Cohen Y, Wang BG, Sidransky D, Kurman RJ, et al. **Mutations in BRAF and KRAS characterize the development of low-grade ovarian serous carcinoma**. *J Natl Cancer Inst*. 2003;95:484-486.
4. Auner V, Kriegshauser G, Tong D, Horvat R, Reinthaller A, Mustea A, et al. **KRAS mutation analysis in ovarian samples using a high sensitivity biochip assay**. *BMC Cancer*. 2009;9:111.
5. Bast RC, Jr., Hennessy B, Mills GB. **The biology of ovarian cancer: new opportunities for translation**. *Nat Rev Cancer*. 2009;9:415-428.
6. Hers I, Vincent EE, Tavare JM. **Akt signalling in health and disease**. *Cell Signal*. 2011;23:1515-1527.
7. Hannan KM, Brandenburger Y, Jenkins A, Sharkey K, Cavanaugh A, Rothblum L, et al. **mTOR-dependent regulation of ribosomal gene transcription requires S6K1 and is mediated by phosphorylation of the carboxy-terminal activation domain of the nucleolar transcription factor UBF**. *Mol Cell Biol*. 2003;23:8862-8877.
8. Wullschleger S, Loewith R, Hall MN. **TOR signaling in growth and metabolism**. *Cell*. 2006;124:471-484.
9. Downward J. **Targeting RAS signalling pathways in cancer therapy**. *Nat Rev Cancer*. 2003;3:11-22.
10. Friday BB, Adjei AA. **Advances in targeting the Ras/Raf/MEK/Erk mitogen-activated protein kinase cascade with MEK inhibitors for cancer therapy**. *Clin Cancer Res*. 2008;14:342-346.
11. Chapman MS, Miner JN. **Novel mitogen-activated protein kinase kinase inhibitors**. *Expert Opin Investig Drugs*. 2011;20:209-220.
12. Sheppard KE, Kinross KM, Solomon B, Pearson RB, Phillips WA. **Targeting PI3 kinase/AKT/mTOR signaling in cancer**. *Crit Rev Oncog*. 2012;17:69-95.
13. Shah OJ, Wang Z, Hunter T. **Inappropriate activation of the TSC/Rheb/mTOR/S6K cassette induces IRS1/2 depletion, insulin resistance, and cell survival deficiencies**. *Curr Biol*. 2004;14:1650-1656.
14. Cheng H, Bagrodia S, Bailey S, Edwards M, Hoffman J, Hu Q, et al. **Discovery of the highly potent PI3K/mTOR dual inhibitor PF-04691502 through structure based drug design**. *Med Chem Commun*. 2010;1:139-144.
15. (http://www.clinicaltrials.gov).
16. LoRusso PM, Krishnamurthi SS, Rinehart JJ, Nabell LM, Malburg L, Chapman PB, et al. **Phase I pharmacokinetic and pharmacodynamic study of the oral MAPK/ERK kinase inhibitor PD-0325901 in patients with advanced cancers**. *Clin Cancer Res*. 2010;16:1924-1937.
17. Wallace EM, Lyssikatos JP, Yeh T, Winkler JD, Koch K. **Progress towards therapeutic small molecule MEK inhibitors for use in cancer therapy**. *Curr Top Med Chem*. 2005;5:215-229.

18. Brown AP, Carlson TC, Loi CM, Graziano MJ. **Pharmacodynamic and toxicokinetic evaluation of the novel MEK inhibitor, PD0325901, in the rat following oral and intravenous administration**. *Cancer Chemother Pharmacol*. 2007;59:671-679.
19. Chou TC. **Drug combination studies and their synergy quantification using the Chou-Talalay method**. *Cancer Res*. 2010;70:440-446.
20. Smyth GK, Michaud J, Scott HS. **Use of within-array replicate spots for assessing differential expression in microarray experiments**. *Bioinformatics*. 2005;21:2067-2075.
21. Kinross KM, Brown DV, Kleinschmidt M, Jackson S, Christensen J, Cullinane C, et al. **In Vivo Activity of Combined PI3K/mTOR and MEK Inhibition in a KrasG12D;Pten Deletion Mouse Model of Ovarian Cancer**. *Mol Cancer Ther*. 2011;10:1440-1449.
22. Subramanian A, Tamayo P, Mootha VK, Mukherjee S, Ebert BL, Gillette MA, et al. **Gene set enrichment analysis: a knowledge-based approach for interpreting genome-wide expression profiles**. *Proc Natl Acad Sci USA*. 2005;102:15545-15550.
23. Hoeflich KP, O'Brien C, Boyd Z, Cavet G, Guerrero S, Jung K, et al. **In vivo antitumor activity of MEK and phosphatidylinositol 3-kinase inhibitors in basal-like breast cancer models**. *Clin Cancer Res*. 2009;15:4649-4664.
24. Liu J, Yang G, Thompson-Lanza JA, Glassman A, Hayes K, Patterson A, et al. **A genetically defined model for human ovarian cancer**. *Cancer Res*. 2004;64:1655-1663.
25. Pende M, Um SH, Mieulet V, Sticker M, Goss VL, Mestan J, et al. **S6K1(-/-)/S6K2(-/-) mice exhibit perinatal lethality and rapamycin-sensitive 5'-terminal oligopyrimidine mRNA translation and reveal a mitogen-activated protein kinase-dependent S6 kinase pathway**. *Mol Cell Biol*. 2004;24:3112-3124.
26. Paez JG, Janne PA, Lee JC, Tracy S, Greulich H, Gabriel S, et al. **EGFR mutations in lung cancer: correlation with clinical response to gefitinib therapy**. *Science*. 2004;304:1497-1500.
27. Serra V, Markman B, Scaltriti M, Eichhorn PJA, Valero V, Guzman M, et al. **NVP-BEZ235, a dual PI3K/mTOR inhibitor, prevents PI3K signaling and inhibits the growth of cancer cells with activating PI3K mutations**. *Cancer research*. 2008;68:8022-8030.
28. Ihle NT, Lemos R, Jr., Wipf P, Yacoub A, Mitchell C, Siwak D, et al. **Mutations in the phosphatidylinositol-3-kinase pathway predict for antitumor activity of the inhibitor PX-866 whereas oncogenic Ras is a dominant predictor for resistance**. *Cancer Res*. 2009;69:143-150.
29. She QB, Chandarlapaty S, Ye Q, Lobo J, Haskell KM, Leander KR, et al. **Breast tumor cells with PI3K mutation or HER2 amplification are selectively addicted to Akt signaling**. *PLoS ONE*. 2008;3:e3065.
30. Dan S, Okamura M, Seki M, Yamazaki K, Sugita H, Okui M, et al. **Correlating phosphatidylinositol 3-kinase inhibitor efficacy with signaling pathway status: in silico and biological evaluations**. *Cancer research*. 2010;70:4982-4994.
31. Garon EB, Finn RS, Hosmer W, Dering J, Ginther C, Adhami S, et al. **Identification of common predictive markers of in vitro response to the Mek inhibitor selumetinib (AZD6244; ARRY-142886) in human breast cancer and non-small cell lung cancer cell lines**. *Mol Cancer Ther*. 2010;9:1985-1994.
32. Solit DB, Garraway LA, Pratilas CA, Sawai A, Getz G, Basso A, et al. **BRAF mutation predicts sensitivity to MEK inhibition**. *Nature*. 2006;439:358-362.
33. Yeh JJ, Routh ED, Rubinas T, Peacock J, Martin TD, Shen XJ, et al. **KRAS/BRAF mutation status and ERK1/2 activation as biomarkers for MEK1/2 inhibitor therapy in colorectal cancer**. *Mol Cancer Ther*. 2009;8:834-843.
34. Nakayama N, Nakayama K, Yeasmin S, Ishibashi M, Katagiri A, Iida K, et al. **KRAS or BRAF mutation status is a useful predictor of sensitivity to MEK inhibition in ovarian cancer**. *Br J Cancer*. 2008;99:2020-2028.

35. Torbett NE, Luna-Moran A, Knight ZA, Houk A, Moasser M, Weiss W, et al. **A chemical screen in diverse breast cancer cell lines reveals genetic enhancers and suppressors of sensitivity to PI3K isoform-selective inhibition**. *Biochem J*. 2008;415:97-110.
36. Engelman JA, Chen L, Tan X, Crosby K, Guimaraes AR, Upadhyay R, et al. **Effective use of PI3K and MEK inhibitors to treat mutant Kras G12D and PIK3CA H1047R murine lung cancers**. *Nat Med*. 2008;14:1351-1356.
37. Hanrahan AJ, Schultz N, Westfal ML, Sakr RA, Giri DD, Scarperi S, et al. **Genomic complexity and AKT dependence in serous ovarian cancer**. *Cancer Discov*. 2012;2:56-67.
38. Meloche S, Pouyssegur J. **The ERK1/2 mitogen-activated protein kinase pathway as a master regulator of the G1- to S-phase transition**. *Oncogene*. 2007;26:3227-3239.
39. Yuan J, Mehta PP, Yin M-J, Sun S, Zou A, Chen J, et al. **PF-04691502, a potent and selective oral inhibitor of PI3K and mTOR kinases with antitumor activity**. *Mol Cancer Ther*. 2011.
40. Rodrik-Outmezguine, Rosen. **mTOR Kinase Inhibition Causes Feedback-Dependent Biphasic Regulation of AKT Signaling**. *Cancer Discovery*. 2011;1-13.

Figure Legends:

Figure 1. Sensitivity of ovarian cancer cells to PF502 and PD901.

Cell proliferation GI50 values (mean ± SEM, n≥3) for a panel of ovarian cancer cell lines treated with either PF502 (A) or PD901 (B). Percent cell death following treatment with either 1μM PF502 (C) or 1μM PD901 (D) for 72hrs. Cell death was determined for all cell lines in response to PF502 and for a subset of PD901 sensitive and resistant cell lines. Each bar represents the average of at least 2 independent experiments.

Figure 2. PF502 is a more potent inhibitor of the PI3K/mTOR pathway in sensitive compared to resistant cells.

A, Five PF502 sensitive (blue bars) and 8 resistant cells (green bars) were treated for 1hr with vehicle, 100nM PF502 (first bar) or 1μM PF502 (second bar). Following immunoblotting, phosphorylated proteins were quantitated by densitometry and then expressed as a percent of the control (DMSO). Each bar represents the mean of at least 2 biological repeats. B, representative immunoblots of a selection of the ovarian cell lines treated with PF502.

Figure 3. PD901 inhibits ERK phosphorylation in both sensitive and resistant cells.

P-ERK and total ERK immunoblots of a subset of PD901 sensitive (A) and resistant cell lines (B) after treatment for 1hr with vehicle (DMSO), 100nM PD901 or 1μM PD901.

Figure 4. Mutations in and protein expression of components of the PI3K/mTOR and RAS/ERK pathways.

A, cell lines are in order of their sensitivity to PF502. Illustrated are activating mutations in PIK3CA (blue) and RAS/RAF (green). B, heat map of expression of PTEN protein and phosphorylated proteins in exponentially growing cells. The levels of PTEN protein, P-PRAS, P-rpS6 and P-ERK1/2 were quantitated from immunoblots as described in Materials and Methods. Numbers and colors represent percent of HOSE cell expression and are the average of at least two biological repeats.

Figure 5. A Combination of PF502 and PD901 synergistically inhibits proliferation of PF502 resistant cells.

A, Combination Index of a subset of PF502 sensitive (open square) and resistant (closed square) cell lines. A combination index of CI<1 indicates synergy, CI>1 indicates

antagonism, and CI=1 indicates additive effect. Shown are the mean ± SEM of at least 3 independent experiments for each cell line. B, representative PF502 dose response curves in the absence (open circles) or presence (closed circles) of 100nM PD901. Dose response curves for PF502 only, were corrected for vehicle treatment control and the combination were corrected for response in the presence of 100nM PD901. C, Cell death in response to 72h treatment with 1μM PF502 (grey bar), 1μM PD901 (white bar) or their combination (black bar). Single agent PD901 response is stacked onto PF502 response whilst the combined treatment is shown as a single bar. Shown is the mean of at least 2 independent experiments for each cell line.

Figure 6. *In vivo* effects of PF502 and PD901 as single agents and in combination on ES2 xenograft tumour growth and PI3K/mTOR signalling.

ES2 tumour bearing mice were treated daily with vehicle, 7.5 mg/kg PF502, 1 mg/kg PD901 or PF502 and PD901 in combination. A, Tumour volume graphed as mean ± SEM, n=9-10. ANOVA, followed by Turkeys' multiple comparison test. *, $p < 0.0001$ between each other for all treatments at 19 days. B, Immunoblot of tumours harvested 4 hours after mice were injected with single dose of vehicle control, PF502, PD901 or their combination.

Sheppard Figure 1

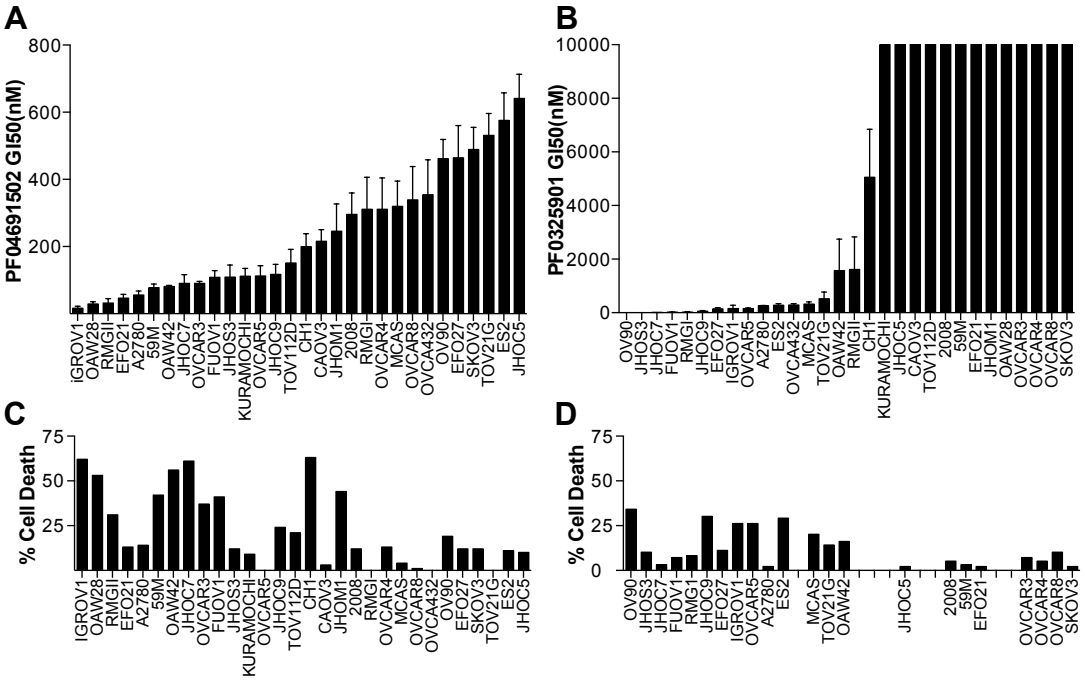

Sheppard Figure 2

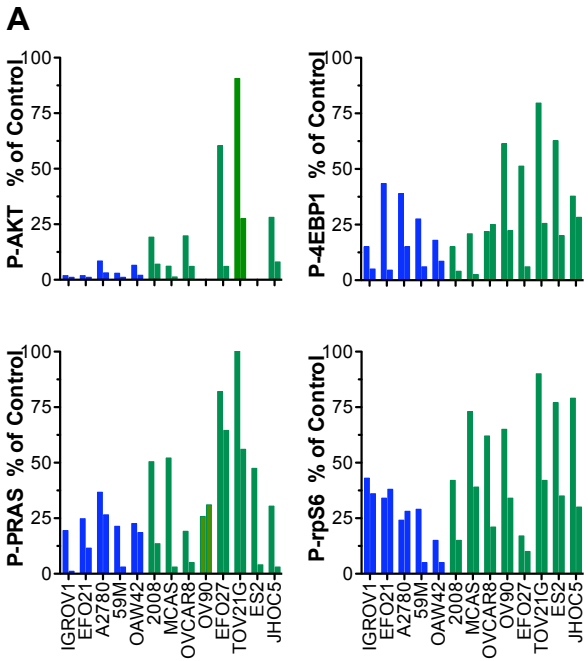

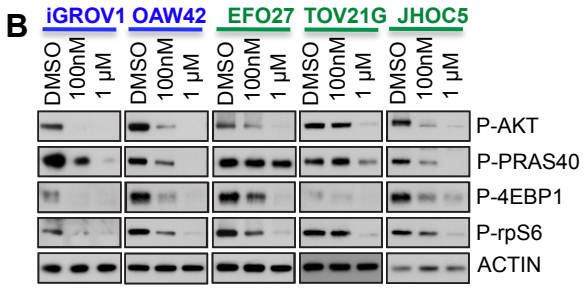

Sheppard Figure 3

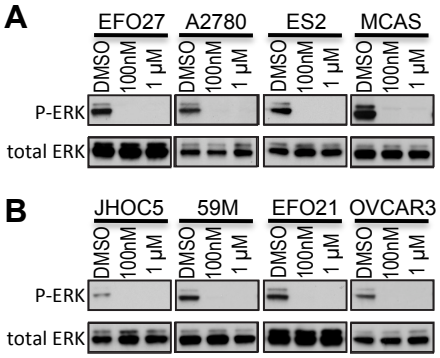

Sheppard Figure 4

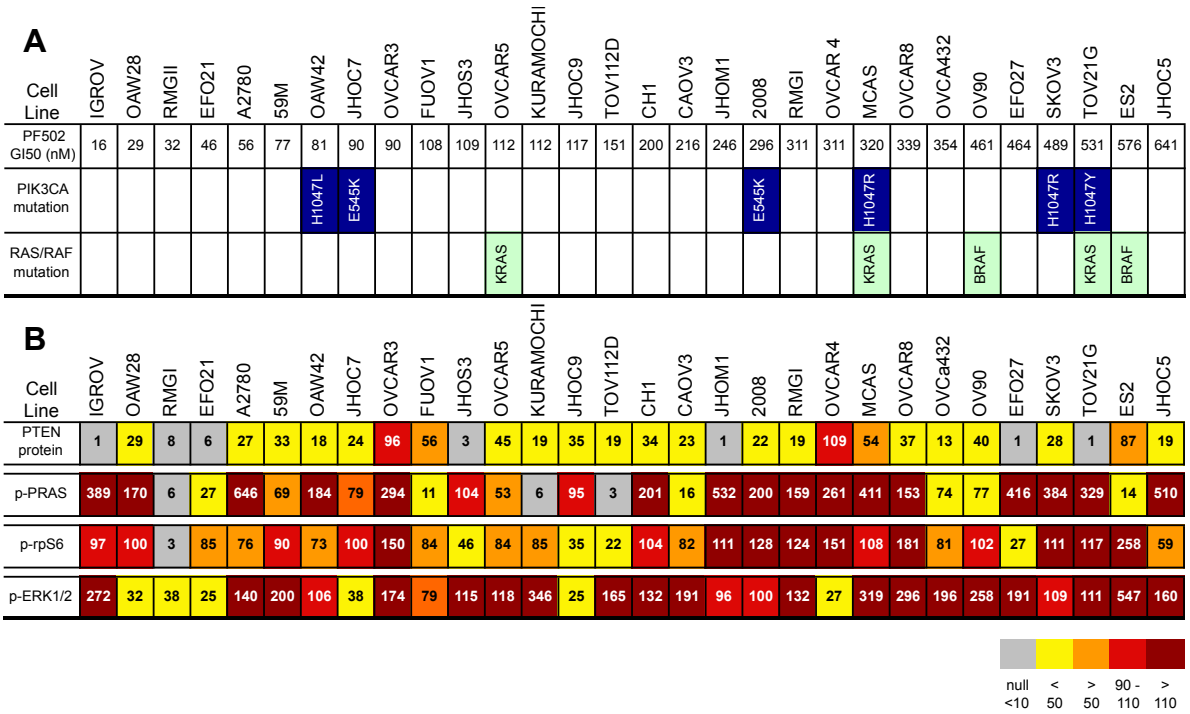

Sheppard Figure 5

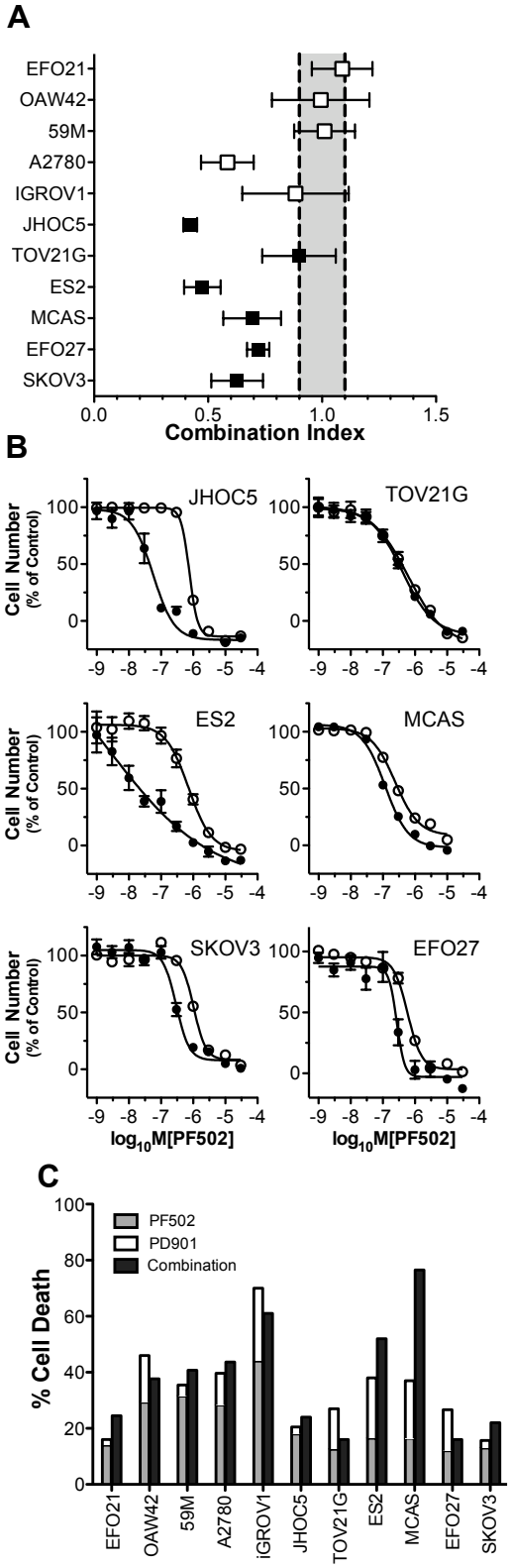

Sheppard Figure 6

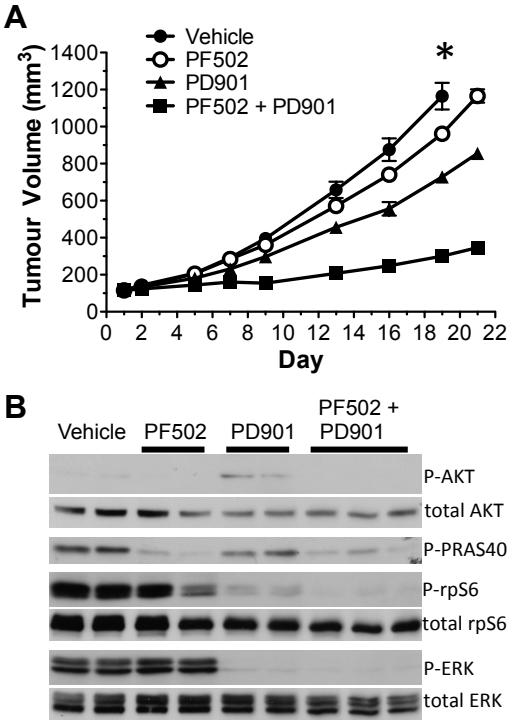

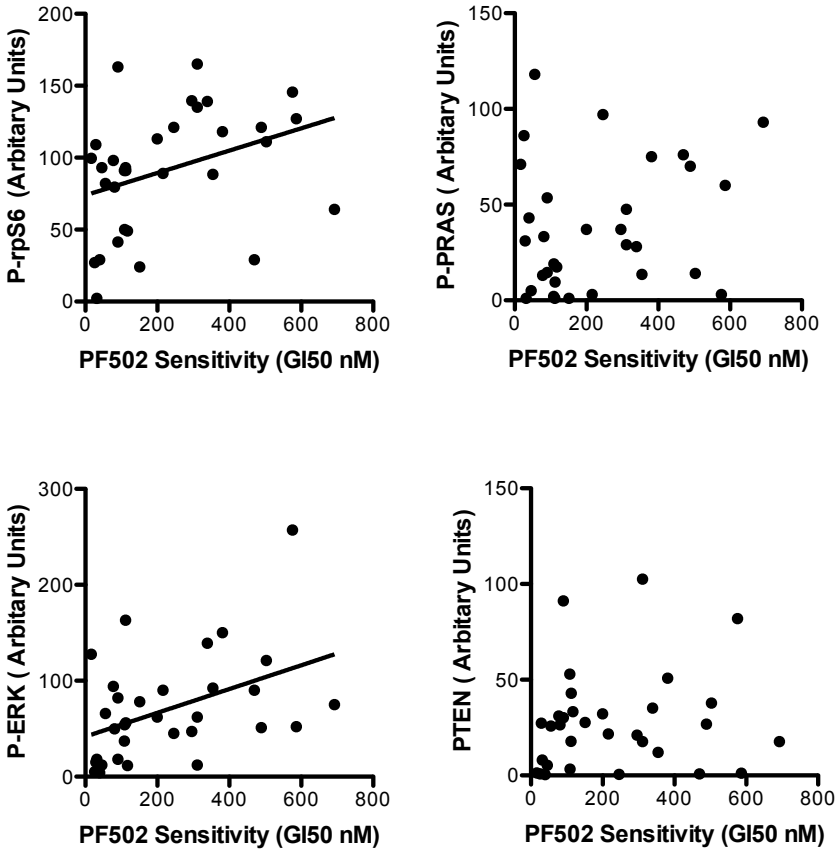

Supplementary Figure S1: Correlation between PF502 sensitivity and components of the PI3K and RAS/ERK pathway

Each dot represents a single cell line where both sensitivity to PF502 and levels of PTEN protein, P-PRAS, P-rpS6 and P-ERK1/2 were quantitated as described in Materials and Methods. A significant correlation was observed between P-rpS6 and PF502 sensitivity and also P-ERK and PF502 sensitivity (Pearson's Correlation: $p < 0.05$) but not with P-PRAS and PTEN.

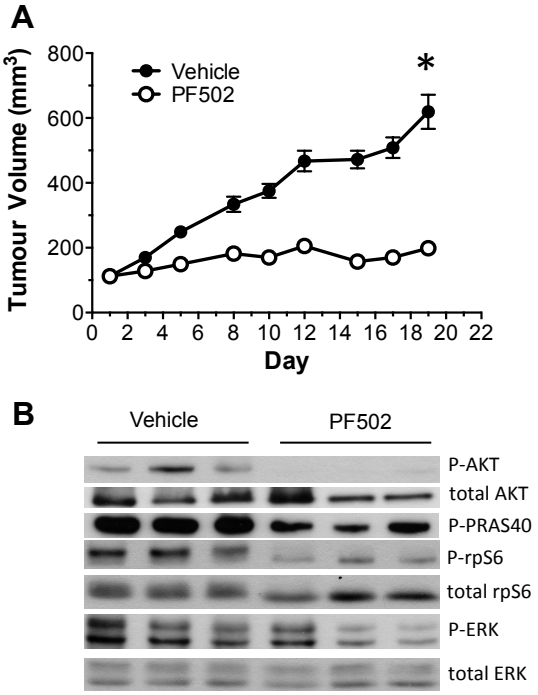

Supplementary Figure S2: *In vivo* effects of PF502 as a single agent on MCAS xenograft tumour growth and PI3K/mTOR signalling.
MCAS tumour bearing mice were treated daily with vehicle, 10 mg/kg PF502. A, Tumour volume graphed as mean ± SEM, n=9-10. Unpaired t test. *, $p < 0.0001$. B, Immunoblot of tumours harvested at 19 days.

Supplementary Table S1: Ovarian cancer cell lines and their corresponding histotype and source

Cell Line	Histotype	Source
2008	Endometrioid	Stephen Howell at University of California, San Diego
59M	Endometrioid	European Collection of Cell Cultures
A2780	mixed histology	European Collection of Cell Cultures
CAOV3	Serous	National Cancer Institute
CH1	Serous	Lloyd Kelland at the Institute of Cancer Research, Sutton, UK
EFO21	Serous	Deutsche Sammlung von Mikroorganismen und Zellkuturen
EFO27	Mucinous	Deutsche Sammlung von Mikroorganismen und Zellkuturen
ES2	Clear Cell	American Type Culture Collection
FUOV1	Serous	Deutsche Sammlung von Mikroorganismen und Zellkuturen
iGROV	Serous	National Cancer Institute
JHOC5	Clear Cell	RIKEN
JHOC7	Clear Cell	RIKEN
JHOC9	Clear Cell	RIKEN
JHOM1	Mucinius	RIKEN
JHOS3	Serous	RIKEN
KURAMOCHI	Unknown	Health Science Research Resources Bank
MCAS	Mucinous	Health Science Research Resources Bank
OAW28	Serous	European Collection of Cell Cultures
OAW42	Serous	European Collection of Cell Cultures
OV90	Serous	American Type Culture Collection
OVCA432	Serous	Dr Nuzhat Ahmed at the Womens Cancer Research Centre, Royal Women's Hospital, Melbourne
OVCAR3	Serous	National Cancer Institute
OVCAR4	Serous	National Cancer Institute
OVCAR5	Unknown	National Cancer Institute
OVCAR8	Serous	National Cancer Institute
RMGI	Clear Cell	Health Science Research Resources Bank
RMGII	Clear Cell	Health Science Research Resources Bank
SKOV3	Serous	National Cancer Institute
TOV112D	Endometrioid	American Type Culture Collection
TOV21G	Clear Cell	American Type Culture Collection

Supplementary Table S2: Primers and annealing temperatures used to amplify targets for sequencing BRAF and KRAS

Target	**Forward primer (5'-3')**	**Reverse primer (5'-3')**	**Annealing Temperature (°C)**
BRAF exon 15	ctaaactcttcataatgcttgctct	ccacaaaatggatccagacaactgttca	65
PIK3CA exon 9	ctgtgaatccagaggggaaa	gtcacaggtaagtgctaaaatg	60
PIK3CA exon 20	cgacagcatgccaatctctt	cagtgtggaatccagagtgagct	60
KRAS exon 2	ggcctgctgaaaatgactga	gtcctgcaccagtaatatgc	60
KRAS exon 3	tcaagtcctttgcccatttt	tgcatggcattagcaaagac	60

Supplementary Table S3 : GSEA analysis of differentially expressed genes between PF502 resistant and sensitive cells

RANKING	ENRICHED IN PF502 RESISTANT	SIZE	ES	FDR q-val
1	CHARAFE BREAST CANCER LUMINAL VS BASAL DN	432	0.71	0.000
2	CHARAFE BREAST CANCER LUMINAL VS MESENCHYMAL DN	435	0.67	0.000
3	RAS ONCOGENIC SIGNATURE UP	174	0.71	0.000
4	HUANG DASATINIB RESISTANCE UP	74	0.79	0.000
5	RICKMAN TUMOR DIFFERENTIATED WELL VS MODERATELY DN	108	0.74	0.000
6	SENESE HDAC1 TARGETS UP	424	0.63	0.000
7	RICKMAN TUMOR DIFFERENTIATED WELL VS POORLY DN	356	0.62	0.000
8	HINATA NFKB TARGETS FIBROBLAST UP	66	0.75	0.000
9	REN ALVEOLAR RHABDOMYOSARCOMA DN	398	0.60	0.000
10	BASAKI YBX1 TARGETS UP	271	0.62	0.000
11	RUIZ TNC TARGETS DN	138	0.66	0.000
12	SENESE HDAC1 AND HDAC2 TARGETS UP	218	0.63	0.000
13	BILD HRAS ONCOGENIC SIGNATURE	242	0.61	0.000
14	AMIT EGF RESPONSE 480 HELA	155	0.63	0.000

RANKING	ENRICHED IN PF502 SENSITIVE	SIZE	ES	FDR q-val
1	NAKAYAMA SOFT TISSUE TUMORS PCA1 DN	77	-.71	0.000
2	NIKOLSKY BREAST CANCER 19Q13.1 AMPLICON	22	-.87	0.000
3	CHARAFE BREAST CANCER LUMINAL VS MESENCHYMAL UP	412	-.54	0.000
4	RICKMAN TUMOR DIFFERENTIATED WELL VS POORLY UP	225	-.56	0.000
5	REACTOME AMINE COMPOUND SLC TRANSPORTERS	25	-.76	0.004
6	BECKER TAMOXIFEN RESISTANCE UP	40	-.68	0.012
7	RICKMAN HEAD AND NECK CANCER A	87	-.58	0.013
8	KOBAYASHI EGFR SIGNALING 24HR UP	99	-.56	0.012
9	CORRE MULTIPLE MYELOMA DN	59	-.61	0.012
10	RICKMAN HEAD AND NECK CANCER B	50	-.61	0.021
11	EINAV INTERFERON SIGNATURE IN CANCER	27	-.69	0.028
12	REACTOME MYOGENESSIS	29	-.69	0.027
13	KUUSELO PANCREATIC CANCER 19Q13 AMPLIFICATION	25	-.69	0.033
14	WU ALZHEIMER DISEASE DN	14	-.80	.050

Top fourteen gene sets enriched in PF502 resistant and sensitive cell lines are shown. Size refers to the number of genes in the gene set and ES is the enrichment score that reflects the degree to which a gene in the gene set is over represented at the extremes (top or bottom) of our differentially expressed ranked list. FDR, is the false discovery rate.

Supplementary Table S4 : GSEA analysis of differentially expressed genes between PD901 resistant and sensitive cells

	ENRICHED IN PD901 RESISTANT	SIZE	ES	FDR q-val
1	NIKOLSKY BREAST CANCER 8Q23 Q24 AMPLICON	146	0.62	0.000
2	VALK AML CLUSTER 2	29	0.78	0.000
3	NIKOLSKY BREAST CANCER 8Q12 Q22 AMPLICON	122	0.57	0.001
4	BASAKI YBX1 TARGETS DN	345	0.47	0.020
5	SCHUETZ BREAST CANCER DUCTAL INVASIVE DN	84	0.55	0.038
6	NIKOLSKY BREAST CANCER 1Q21 AMPLICON	37	0.64	0.037
7	CHARAFE BREAST CANCER LUMINAL VS MESENCHYMAL UP	412	0.44	0.072
8	HALMOS CEBPA TARGETS DN	39	0.59	0.091
9	TSAI DNAJB4 TARGETS UP	13	0.77	0.084
10	REACTOME AMINE COMPOUND SLC TRANSPORTERS	25	0.67	0.084
11	KUUSELO PANCREATIC CANCER 19Q13 AMPLIFICATION	25	0.67	0.082
12	NIKOLSKY BREAST CANCER 7P15 AMPLICON	11	0.81	0.093
13	SMID BREAST CANCER RELAPSE IN BRAIN UP	38	0.61	0.092
14	REACTOME CELL CELL ADHESION SYSTEMS	58	0.56	0.098

	ENRICHED IN PD901 SENSITIVE	SIZE	ES	FDR q-val
1	CHARAFE BREAST CANCER LUMINAL VS BASAL DN	432	-.57	0.000
2	RICKMAN TUMOR DIFFERENTIATED WELL VS POORLY DN	356	-.56	0.000
3	RICKMAN TUMOR DIFFERENTIATED WELL VS MODERATELY DN	108	-.65	0.000
4	RAS ONCOGENIC SIGNATURE UP	174	-.60	0.000
5	CHARAFE BREAST CANCER LUMINAL VS MESENCHYMAL DN	435	-.52	0.000
6	REN ALVEOLAR RHABDOMYOSARCOMA DN	398	-.53	0.000
7	BASAKI YBX1 TARGETS UP	271	-.55	0.000
8	BILD HRAS ONCOGENIC SIGNATURE	242	-.54	0.000
9	WU CELL MIGRATION	183	-.54	0.001
10	NAKAMURA METASTASIS MODEL DN	41	-.67	0.003
11	XU HGF SIGNALING NOT VIA AKT1 6HR	24	-.75	0.003
12	REACTOME TELOMERE MAINTENANCE	72	-.59	0.003
13	BRUECKNER TARGETS OF MIRLET7A3 DN	71	-.60	0.003
14	KEGG COMPLEMENT AND COAGULATION CASCADES	67	-.60	0.004

Top fourteen gene sets enriched in PD901 resistant and sensitive cell lines. Size refers to the number of genes in the gene set and ES is the enrichment score that reflects the degree to which a gene in the gene set is over represented at the extremes (top or bottom) of our differentially expressed ranked list. FDR, is the false discovery rate.

Supplementary Table S5 : GeneGo Pathway analysis of differentially expressed genes between PF502 resistant and sensitive cells. Pathways that were significantly enriched (FDR 0.05)

	PATHWAYS ENRICHED IN PF502 RESISTANT
1	Cell adhesion ECM remodeling
2	Cell adhesion Chemokines and adhesion
3	Immune response IL-18 signaling
4	Immune response HMGB1/RAGE signaling pathway
5	Development Regulation of epithelial-to-mesenchymal transition (EMT)
6	Immune response IL-17 signaling pathways
7	Immune response Oncostatin M signaling via MAPK in human cells
8	Development TGF-beta-dependent induction of EMT via MAPK
9	Development EGFR signaling pathway
10	Development ERBB-family signaling

	PATHWAYS ENRICHED IN PF502 SENSITIVE
1	Cell adhesion ECM remodeling
2	Development WNT signaling pathway. Part 2
3	Cytoskeleton remodeling TGF, WNT and cytoskeletal remodeling
4	Development Regulation of epithelial-to-mesenchymal transition (EMT)
5	Cell adhesion Tight junctions
6	GTP metabolism

	PATHWAYS ENRICHED IN PD901 RESISTANT
1	Development TGF-beta-dependent induction of EMT via SMADs
2	Development Regulation of epithelial-to-mesenchymal transition (EMT)

	PATHWAYS ENRICHED IN PD901 SENSITIVE
1	Blood coagulation Blood coagulation
2	Cell adhesion ECM remodeling
3	Retinol metabolism
4	Cell adhesion PLAU signaling
5	Transcription Role of VDR in regulation of genes involved in osteoporosis
6	Normal and pathological TGF-beta-mediated regulation of cell proliferation
7	Signal transduction Erk Interactions: Inhibition of Erk
8	Cell adhesion Cell-matrix glycoconjugates
9	Development ERBB-family signaling
10	Development Regulation of epithelial-to-mesenchymal transition (EMT)

Pathways that had a false discovery rate (FDR) of less than 5% percent were considered significant. There were 82 pathways enriched in PF502 resistant cells of which 10 are shown. All significant pathways enriched in PF502 sensitive , PD901 resistant and PD901 sensitive are shown.

Supplementary Methods:

Immunoblotting

Exponentially growing cells were lysed in RIPA buffer (1mmol/L EDTA; 1% NP40; 0.5% sodium deoxychlorate; 0.1% SDS; 50mmol/L sodium fluoride; 1mmol/L sodium pyrophosphate in PBS) plus phosphatase inhibitor cocktail (Roche). Protein concentrations were determined by DC Protein assay (BioRad). Lysates were subjected to SDS-PAGE, transferred to PDVF, immunoblotted and proteins visualized by Western Lightening Plus Enhanced Chemiluminescence (PerkinElmer) and the band density quantified using ImageQuant TL Software, Version 7.0 (GE Healthcare). Primary antibodies include: p-AKT S473 (Cell Signaling (CS)#4058), pPRAS40 T246 (CS#2997), p-rpS6 S240/244 (CS#2215), p4E-BP1 S65 (CS#9451), pERK T202/Y204 (CS#9106), ERK1 (Santa Cruz-94), actin (MP Biomedicals #691001). Anti-mouse and anti-rabbit horseradish peroxidase-conjugated secondary antibodies were used (BioRad #170-6516, #170-6515).

Author/s:
Sheppard, KE; Cullinane, C; Hannan, KM; Wall, M; Chan, J; Barber, F; Foo, J; Cameron, D; Neilsen, A; Ng, P; Ellul, J; Kleinschmidt, M; Kinross, KM; Bowtell, DD; Christensen, JG; Hicks, RJ; Johnstone, RW; McArthur, GA; Hannan, RD; Phillips, WA; Pearson, RB

Title:
Synergistic inhibition of ovarian cancer cell growth by combining selective PI3K/mTOR and RAS/ERK pathway inhibitors

Date:
2013-12-01

Citation:
Sheppard, K. E., Cullinane, C., Hannan, K. M., Wall, M., Chan, J., Barber, F., Foo, J., Cameron, D., Neilsen, A., Ng, P., Ellul, J., Kleinschmidt, M., Kinross, K. M., Bowtell, D. D., Christensen, J. G., Hicks, R. J., Johnstone, R. W., McArthur, G. A., Hannan, R. D. ,... Pearson, R. B. (2013). Synergistic inhibition of ovarian cancer cell growth by combining selective PI3K/mTOR and RAS/ERK pathway inhibitors. EUROPEAN JOURNAL OF CANCER, 49 (18), pp.3936-3944. https://doi.org/10.1016/j.ejca.2013.08.007.